Simulation of Cell Adhesion to Bioreactive Surfaces in Shear: The Effect of Cell Size

David F. J. Tees,[†] Kai-Chien Chang,[‡] Stephen D. Rodgers,[†] and Daniel A. Hammer*[,†,§]

Departments of Chemical Engineering and Bioengineering, University of Pennsylvania, Philadelphia, Pennsylvania 19104, and Department of Chemical Engineering, Cornell University, Ithaca, New York 14853

Leukocyte adhesion under flow in the microvasculature is a multistep process in which rolling adhesion is followed by firm arrest. These interactions are mediated by binding between receptors on the leukocyte surface and complementary ligands on the surface of endothelial cells. Previous work using a computational method called "adhesive dynamics" showed that the general shape of a state diagram for cell adhesive behavior in flow could be predicted by the bond reaction rates and their dependence on force. Other parameters, however, such as shear rate, particle size, and receptor and ligand density, determined the exact region of parameter space that corresponds to an adhesive behavior. In this paper, we present state diagrams for adhesion for a range of particle sizes to explain the rolling behavior for a wide range of cell diameters. Particle size is an easily controlled experimental variable, and if the locations of regions of desired adhesive behavior in the state diagram are known, then the size of particle needed to achieve a desired adhesive behavior can be predicted.

Introduction

The adhesion of blood-borne cells to blood vessel walls is a crucial factor in inflammation, lymphocyte homing, and cancer metastasis. Over the past decade, it has been demonstrated that several steps are required for firm arrest of leukocytes and other cell types on vascular endothelial cells and that these steps are mediated by distinct sets of adhesion molecules.[1] Initial tethering and transient "rolling" adhesion are both primarily mediated by the selectin family of adhesion molecules binding to their carbohydrate ligands. Firm arrest of rolling cells is primarily mediated by the integrin family binding to members of the immunoglobulin superfamily. Firm adhesion is usually followed by trans-endothelial migration, so that the cell can carry out its intended function within the tissue.

In previous work, we used a computer simulation of cell adhesion called adhesive dynamics to simulate the initial tethering and rolling process. We found that a state diagram for adhesion could be constructed.[2] The adhesive phenotypes observed fell into three categories. (1) There is a "no adhesion" state for cell attachment in flow similar to that seen for β_2 integrins binding to ICAM-1 at moderate to high flow rates. The cell simply moves over the surface without making any durable adhesive contact. (2) Many antigen−antibody pairs mediate "firm adhesion" under flow,[3,4] characterized by sudden arrest from free-stream motion, followed by durable attachment. (3) Transient or rolling adhesion similar to that seen for selectin-mediated leukocyte rolling also occurs. Experimental confirmation that the dynamics of adhesion is coded by the physical chemistry of adhesion molecules themselves comes from our laboratory's cell-free adhesion experiments.[5−7] We attached the selectin-binding tetrasaccharide sialyl-Lewis^x to inert, rigid polystyrene microspheres and demonstrated that these model leukocytes roll over E-, P-, or L-selectin substrates at velocities comparable to those of real leukocytes.

In the previous work, simulated adhesive behavior was observed as a number of physicochemical properties were varied. Rate of reaction, mechanical elasticity, kinetic response to stress, and length of adhesion molecules were all tested. The dissociation rate of the bond and its dependence on force turned out to be the dominant parameters in determining the shape of the state diagram. This arises from the need for the cell to form a durable attachment in shear; the bonds must thus be able to withstand hydrodynamic stress, particularly at the trailing edge of the contact zone. The dissociation rate will affect the cell's ability to sustain rolling adhesion, and the time scale for bond rupture will set the rolling velocity. Although there are a number of relations describing the force dependence of rates,[8,9] the Bell model[10] has been shown to be a good, simple approximation,[11] and it is widely used in the literature describing cell rolling. The model predicts that the reverse reaction rate, $k_r(f)$, for a bond under applied force f is given by

$$k_r = k_r^o \exp(r_o f/k_b T) \qquad (1)$$

where k_r^o is the unstressed dissociation rate constant, k_bT is the thermal energy, and r_o is a parameter with units of length that relates the reactivity of the molecule to the details of the intermolecular potential of mean force for single bonds. When a force, f, is applied to a bond, the entire potential is "tilted", i.e., rf is subtracted

* Please address correspondence to Dr. Hammer, 120 Hayden Hall, Department of Bioengineering, University of Pennsylvania, Philadelphia, PA 19104. Telephone: (215) 573-6761. Fax: (215) 573-2071. E-mail: hammer@seas.upenn.edu.

[†] Department of Chemical Engineering, University of Pennsylvania.

[‡] Cornell University.

[§] Department of Bioengineering, University of Pennsylvania.

10.1021/ie010383p CCC: $22.00 © 2002 American Chemical Society
Published on Web 12/05/2001

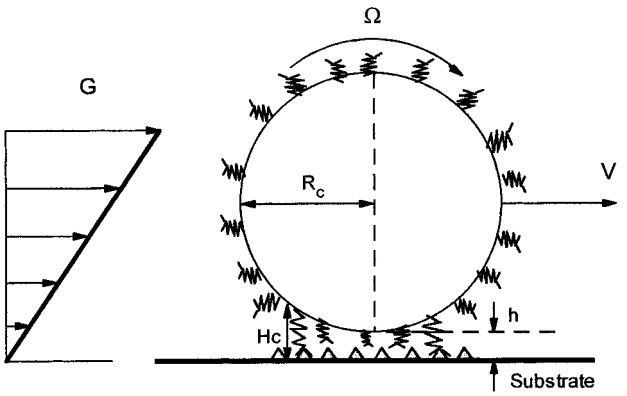

Figure 1. Schematic diagram of adhesive dynamics. A sphere coated with receptors binds to ligands on a flat surface. The separation distance between cell and surface is h. Receptors inside the region defined by H_c are reactive.

from the original potential $E(r)$. This effectively reduces the barrier for unbinding, and depending on the shape of the potential, it might also change the distance to the transition state. If the potential curve has a sharp cusp at the transition state distance, r_o, however, the distance between the potential minimum and the transition state changes little as force is applied (at least for modest forces). The height of the barrier to dissociation is then reduced by $\sim r_o f$ as force is applied.[12,13] This reduction is the origin of the $\exp(r_o f/k_b T)$ term in the Bell model: it represents the change in barrier height for dissociation induced by an applied force for a sharp transition state.

In previous work,[2] we presented state diagrams for adhesion for simulated 10-μm spheres. This size was chosen to match the cell-free rolling experiments described above. Neutrophils, however, are only $\sim$8.5 μm in diameter.[14] It is thus desirable to examine state diagrams for adhesion with different particle sizes to verify that the Bell model parameters measured for the molecules that mediate rolling[15−19] do indeed fall in the rolling region of the state diagram for a more realistic particle size. In addition, several other cell types with a wide range of particle sizes have been observed to exhibit rolling phenotypes. The most notable among these are platelets ($\sim$2 μm in diameter), which can be seen to tumble on selectins or von Willebrand Factor,[20,21] and metastasizing cancer cells (diameters up to $\sim$20 μm), which are also seen to roll.[22,23] In a further application, the particle size is a parameter that is easy to vary in experiments. The ability to recreate particle rolling using colloidal cell mimetics makes it feasible to vary particle size and examine changes in rolling dynamics. The state diagrams presented here should thus be of use both as a means of interpreting rolling and as a guide to the particle size needed to enable rolling adhesion with any given adhesion molecule. In this paper, we present state diagrams for different particle sizes, including leukocyte-sized particles, to address these two issues.

Methods

The adhesive dynamics method (shown schematically in Figure 1) has been extensively described.[2,25−28] The simulation begins with a smooth, rigid, three-dimensional "cell" or receptor-coated particle (modeled as a sphere with receptors distributed at random over its surface) driven over a uniformly reactive surface at a separation distance h that is greater than the length of a receptor−ligand bond by a simple shear flow with wall shear rate G. The cell is allowed to reach a steady separation distance and translational velocity in the absence of specific interactions, after which receptor-mediated binding is initiated. The tip of each free adhesion molecule and the uniformly reactive substrate react with association rate k_f and dissociation rate $k_r(f)$. We use eq 1 to model $k_r(f)$. We assume that k_f (a function of h and the slip velocity, V_s, between the cell and the surface[29]) is equal to its maximum value $k_f^o(V_s)$ provided h is less than a critical separation distance, H_c, and that $k_f = 0$ for $h > H_c$. During a time step, each free receptor inside the reactive region has a probability P_f of forming a tether in the time interval dt[25]

$$P_f = 1 - \exp[-k_f(V_s)\, dt] \tag{2}$$

In the same interval, each currently tethered receptor has the probability P_r of dissociating

$$P_r = 1 - \exp(-k_r\, dt) \tag{3}$$

During each time step, bond formation and breakage are simulated using a Monte Carlo process, in which bond formation and breakage occur if random numbers are chosen that are less than the probabilities P_f and P_r for binding and unbinding, respectively, in the time interval.[26] The bond stresses, f, are calculated from the distance between the end points of the attachment, L, using Hooke's law, $f = \sigma(L - \lambda)$, where σ is the spring constant and λ is the unstressed length of the adhesive complex. The stress contributed by each bond is summed to determine the total force and torque exerted by the bonds on the cell. In addition to the bonding forces, we include colloidal forces[26] and the external force and torque imparted to the cell by fluid shear[30] to compute the net force and torque acting on the cell. The motion of the particle is obtained from the mobility matrix for a sphere near a plane wall in a viscous fluid.[25,26] The new positions of free receptors and tethers at $t + dt$ are updated from their positions at t using the translational and angular velocity of the cell. The process is repeated until the cell travels 0.1 cm or 10 s of simulated time has elapsed.

Results

Adhesive dynamics simulations were performed with a grid of k_r^o and r_o values for $R_c = 5.0$, 3.75, and 2.5 μm. Four equally spaced (on a logarithmic scale) values of the parameters were simulated for each order of magnitude in k_r^o and r_o covering ranges from 10^{-5} s^{-1} $\leq k_r^o \leq 10^5$ s^{-1} and 10^{-2} Å $\leq r_o \leq 10$ Å. The number of receptors, N_r, on the sphere surface was either held constant (with $N_r = 25\,000$ and, hence, receptor density $n_r = 80$, 140, and 320 receptor/μm^2 for $R_c = 5.0$, 3.75, and 2.5 μm, respectively) or was varied to maintain a constant density of 80 receptor/μm^2 (and thus $N_r =$ 25 000, 14 100, and 6250 for $R_c = 5.0$, 3.75, and 2.5 μm, respectively). All other biophysical parameters were held constant. The values for these parameters (given in Table 1) were chosen to be consistent with the cell-free rolling experiments.[28] The simulations used to create the state diagrams were performed at a wall shear rate of 100 s^{-1}. This shear rate is in the center of the range for which leukocyte rolling is observed.[31,32] Rolling is frequently defined in the literature as cell

Table 1. Simulation Parameters

parameter	definition	value
R_p	receptor radius	1.0 nm[a]
N_L	ligand density	3600 cm^{-2} [b]
λ	equilibrium bond length	20 nm[a]
σ	spring constant	100 dyn·cm^{-1} [c]
μ	viscosity	0.01 g·cm^{-1}·s^{-1}
G	wall shear rate	100 s^{-1}
H_c	cutoff length for formation	40 nm
T	temperature	310 K
k_f	association rate	84.0 s^{-1}

[a] Reference 10. [b] Reference 6. [c] Reference 24.

movement that is significantly slower than the unhindered hydrodynamic velocity, V_H.[33] Accordingly, the state diagram results are presented as contour plots of V/V_H for $R_c = 5.0$ μm (Figures 2a and 3a), 3.75 μm (Figures 2b and 3b), and 2.5 μm (Figures 2c and 3c). The V value is the gross average velocity found by dividing the distance traveled during the simulation by the simulation time. Figure 2 shows state diagrams for a constant receptor number N_r (and hence varying receptor density as particle size changes). Figure 3 shows state diagrams for a constant receptor density n_r (and hence varying receptor number as particle size changes).

To create the state diagrams, V/V_H was plotted versus k_r^o for each of the different r_o values used. The k_r^o values for which $V/V_H = 0.95$, 0.5, 0.3, 0.1, 0.05, and 0.0 were estimated from these graphs. The $k_r^o-r_o$ pairs that led to a given V/V_H were connected as lines on the state diagrams. As shown in Figure 2a, the nonadherent region of the state diagram (the region of parameter space that led to particles with $V/V_H > 0.95$) is above and to the right of the thick light blue line. The other lines represent $V/V_H = 0.5$ (dashed line), 0.3, 0.1, 0.05, and 0.0 (dotted line). The region $0.0 < V/V_H < 0.5$ (dotted and dashed lines) can be considered the rolling or transient adhesion region. The $V/V_H = 0.0$ curves (dotted dark blue line) represents the edge of $k_r^o-r_o$ parameter space for which the particle is in motion and, hence, the $0.0V_H$ limit for sudden firm capture from flow. Rolling at $V \geq 0.5V_H$ (dashed purple line) would be taken as the cutoff for rolling adhesion in most assays of leukocyte rolling velocity. The region of $k_r^o-r_o$ space that corresponds to rolling runs largely horizontal as r_o is increased up to $r_o \approx 0.1$ Å and then bends over and plunges steeply toward the r_o axis as r_o is increased further. For small k_r^o and large r_o, the velocity contours for rolling become more closely spaced for all particle sizes. The same trends are observed with all particle sizes for both constant N_r (Figure 2) and constant n_r (Figure 3).

For all particle sizes, the patterns of particle velocity as a function of the Bell model parameters are very similar, but there are subtle shifts in the contours for different particle sizes and receptor density or receptor number. These shifts are shown in Figure 4a and b for contours of $V/V_H = 0.0$ and $V/V_H = 0.5$, respectively. The solid black line represents $R_c = 5.0$ μm (it is the same for constant N_r and constant n_r, and hence, it has been colored black). The dashed lines represent $R_c = 3.75$ μm, and the dotted lines $R_c = 2.5$ μm. When N_r is held constant (blue dashed and dotted lines), the contours for a given V/V_H value shift upward and to the right along both k_r^o and r_o axes for each decrease of 1.25 μm in R_c. The magnitudes of the shifts along the r_o axis are

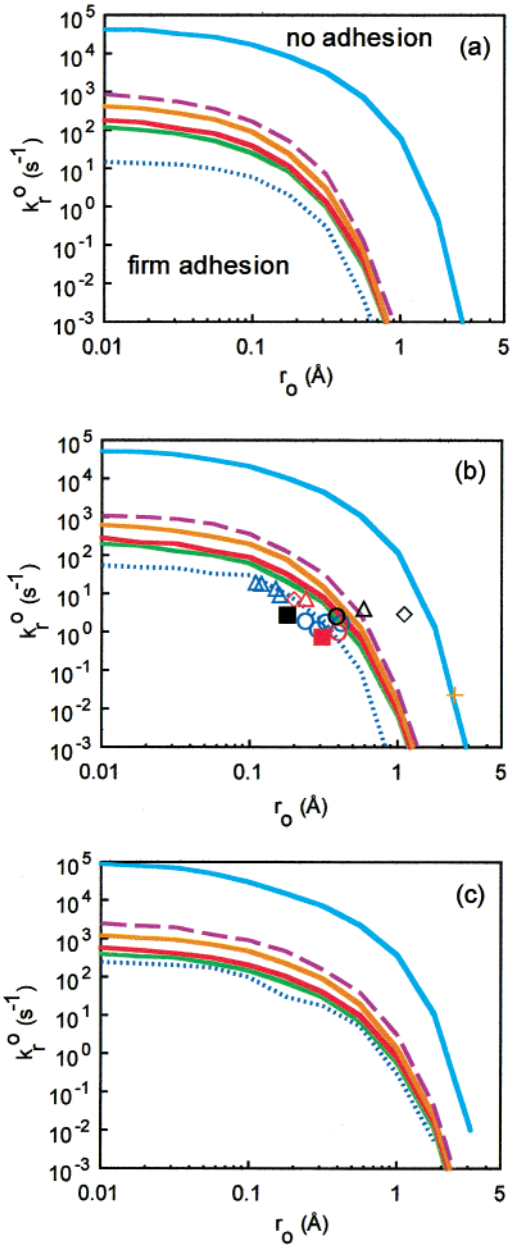

Figure 2. State diagrams for adhesion for R_c = (a) 5.0, (b) 3.75, and (c) 2.5 μm for constant $N_r = 25\,000$. The colors code for the lines of equal V/V_H. The thick light blue line represents $V = 0.95V_H$, purple (dashed line) is $V = 0.5V_H$ (the cutoff speed for the interaction to be considered rolling), orange is $0.3V_H$, red is $0.1V_H$, green is $0.05V_H$, and dark blue (dotted line) is $0.0V_H$ (essentially firm adhesion). The firm adhesion and no adhesion areas are labeled in part a. The locations corresponding to the Bell model parameters measured in the literature for E-selectin (squares),[16,17] P-selectin (circles[15,17,18] and cross[34]), L-selectin (diamonds)[17,18,35], and PNAd (triangles)[16,17] are shown in part b. The parameter values lie near or within the envelope for rolling. The only exception is the P-selectin/PSGL-1 value from atomic force microscopy (cross).[34] The points in red are from the Springer lab,[15,16,35] the points in blue are from the McEver lab,[18] and the points in black are from the Lawrence lab.[17]

very similar for both the rolling versus nonrolling criterion curve ($V/V_H = 0.5$) and the firm adhesion criterion line ($V/V_H = 0.0$), although for $V/V_H = 0.5$, there is only a very small shift in k_r^o. When n_r is held constant (red dashed and dotted lines), however, there is significantly less shift of the boundary curves for the rolling region as R_c varies. The $V/V_H = 0.0$ lines are

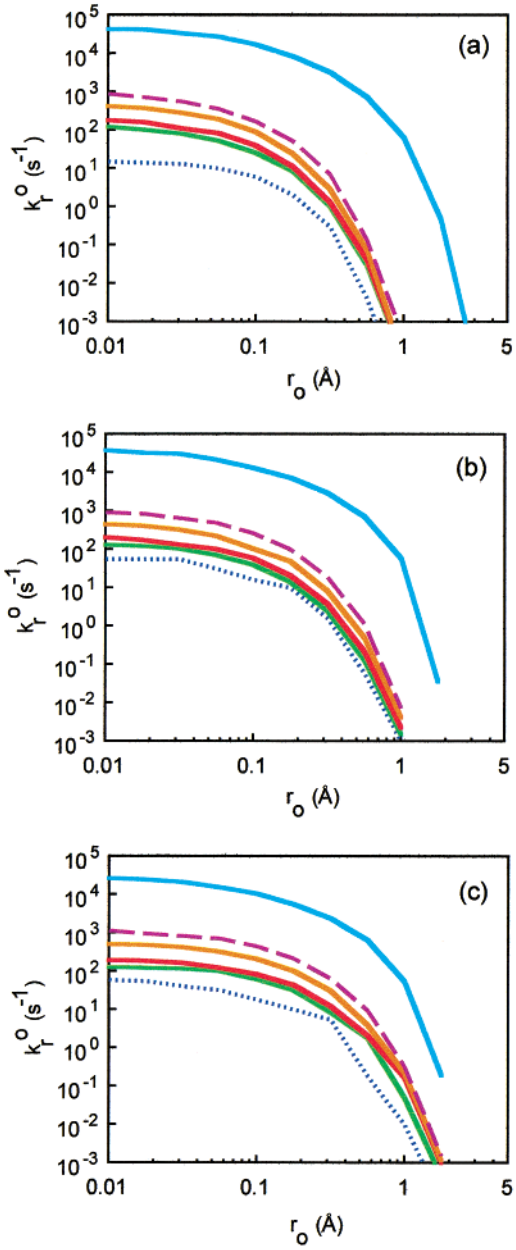

Figure 3. State diagrams for adhesion for R_c = (a) 5.0, (b) 3.75, and (c) 2.5 μm at constant receptor density, n_r = 80 μm^{-2}. The colors code for the lines of equal V/V_H. The thick light blue line represents $V = 0.95V_H$, purple (dashed line) is $V = 0.5V_H$ (the cutoff speed for the interaction to be considered rolling), orange is $0.3V_H$, red is $0.1V_H$, green is $0.05V_H$, and dark blue (dotted line) is $0.0V_H$ (essentially firm adhesion).

shifted very little for R_c = 3.75 and 2.5 μm, and the shifts in the V/V_H = 0.5 lines are not as large as when the receptor number is held constant.

Figure 5a and b shows a set of slices through the constant-N_r state diagrams for R_c = 5.0, 3.75, and 2.5 μm at two values of the Bell model parameter r_o as k_r^o is varied. Figure 5a shows the state diagram cut for r_o = 1.0 Å (somewhat larger than the value found for selectins).[15−19] For small k_r^o, the particles adhere firmly without rolling. As k_r^o increases, the rolling velocity increases in a doubly sigmoidal curve for each of the particle sizes. There is an initial rapid increase in rolling velocity up to $V/V_H \approx 0.6$ and then a much slower increase between $0.6 < V/V_H < 0.8$. There is then another rapid increase to the unbound hydrodynamic

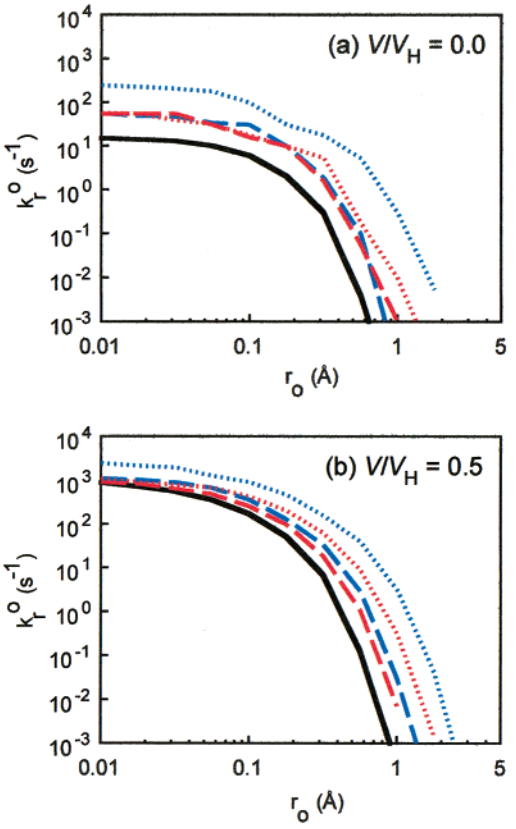

Figure 4. Detailed examination of the effect of R_c on the equal rolling velocity lines for V/V_H = (a) 0.0 (threshold of firm adhesion) and (b) 0.5 (no adhesion cutoff) for R_c = 5.0 μm (solid line), 3.75 μm (dashed line), and 2.5 μm (dotted line). The constant-N_r curves are shown in blue, and the constant-n_r curves are shown in red (except for R_c = 5.0 μm, which is the same for both constant N_r and constant n_r; it has been colored black).

velocity at a k_r^o value between 10 and 100 s^{-1} that varies little with particle size. The k_r^o value for which the rolling velocity begins to increase, however, shifts to higher values of k_r^o as R_c is reduced. For each reduction of 1.25 μm in R_c, there is an almost 2 order of magnitude increase in the k_r^o value at which rolling begins. In contrast, the curves for selectin-like r_o = 0.3 Å (shown in Figure 5b) are closer to single sigmoidal curves (especially for the smaller values of R_c), and the minimum k_r^o value needed for the initiation of rolling varies by only an order of magnitude for the different R_c values. As r_o decreases further (to r_o = 0.1 Å or less), the V/V_H vs k_r^o curves become singly sigmoidal for all R_c, and the k_r^o values for initiation of rolling get even closer together for the different R_c (data not shown).

The state diagrams shown above were all obtained with a wall shear rate of 100 s^{-1}. To examine how the velocities change with shear rate, simulations were run with different R_c values for wall shear rates of 50, 100, 200, 300, and 400 s^{-1} using a constant N_r for all particle sizes. The temperature was also set to 23 °C to more accurately reproduce the value used in in vitro assays. The resulting V/V_H values are plotted in Figure 6 as a function of the shear rate for three sets of Bell model parameters corresponding to those typical for selectin−carbohydrate bonds (Figure 6a, r_o = 0.3 Å and k_r^o = 1 s^{-1}), a typical antibody−antigen bond (Figure 6b, r_o = 1.0 Å and $k_r^o = 10^{-2}$ s^{-1}), and streptavidin−biotin (Figure 6c, r_o = 3.0 Å and $k_r^o = 10^{-4}$ s^{-1}).

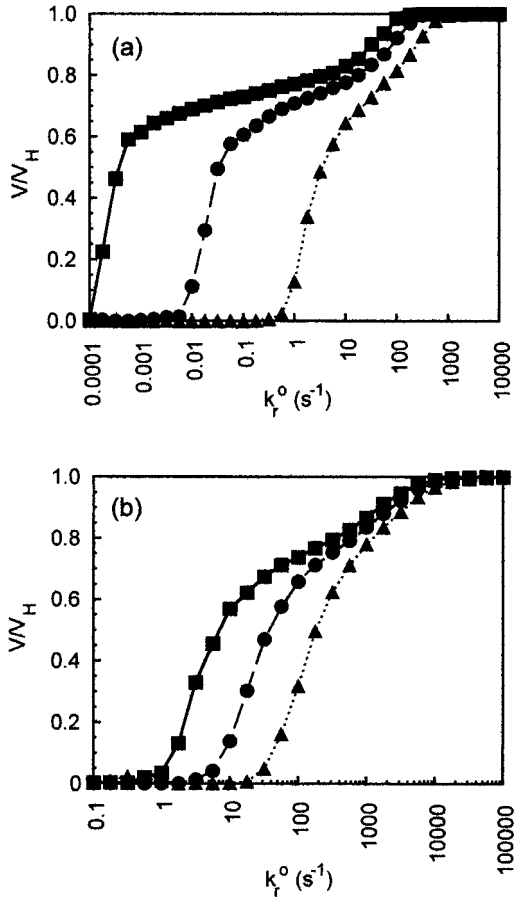

Figure 5. Slices through the state diagrams for different R_c values at constant N_r showing V/V_H as a function of k_r^o for r_o = (a) 1.0 and (b) 0.3 Å. The symbols represent R_c = 5.0 μm (squares, solid line), 3.75 μm (circles, dashed line), and 2.5 μm (triangles, dotted line).

For selectin-like bonds, V/V_H versus shear is shown in Figure 6a for R_c = 2.5, 3.75, and 5.0 μm. The largest spheres roll for shear rates of up to ~100 s^{-1} but become nonadherent at shear rates that are only slightly larger. For the smaller spheres, the slow rolling can continue up to higher values of G. Figure 6b shows similar curves for antibody-like Bell model parameters. For antibody-like bonds, there is wider range of shear rate over which interaction is possible, but adhesion tends to be either sudden capture or nonexistent at most shear rates and particle sizes. For streptavidin-like bonds (Figure 6c), the particles are either nonadherent or firmly bound at all shear rates. The range of shear rate over which particles coated with streptavidin can roll is thus extremely narrow or only occurs for bead size smaller than 2.5 μm in radius. It is interesting to note that, in most cases, the particles deemed by convention to be "nonadherent" actually move at velocities significantly less than the hydrodynamic velocity (although still faster than the $V/V_H > 0.5$ threshold for rolling). There are a few adhesive interactions for these particles but not enough to slow the particle sufficiently to be counted as rolling.

The data from Figure 6a–c are replotted in Figure 7 with V/V_H shown versus R_c for G = 50, 100, 200, and 400 s^{-1} (and constant N_r). As with Figure 6, this plot shows that, as R_c is varied, it is possible to have adhesive behavior change from firm adhesion to rolling to no adhesion as particle size is increased.

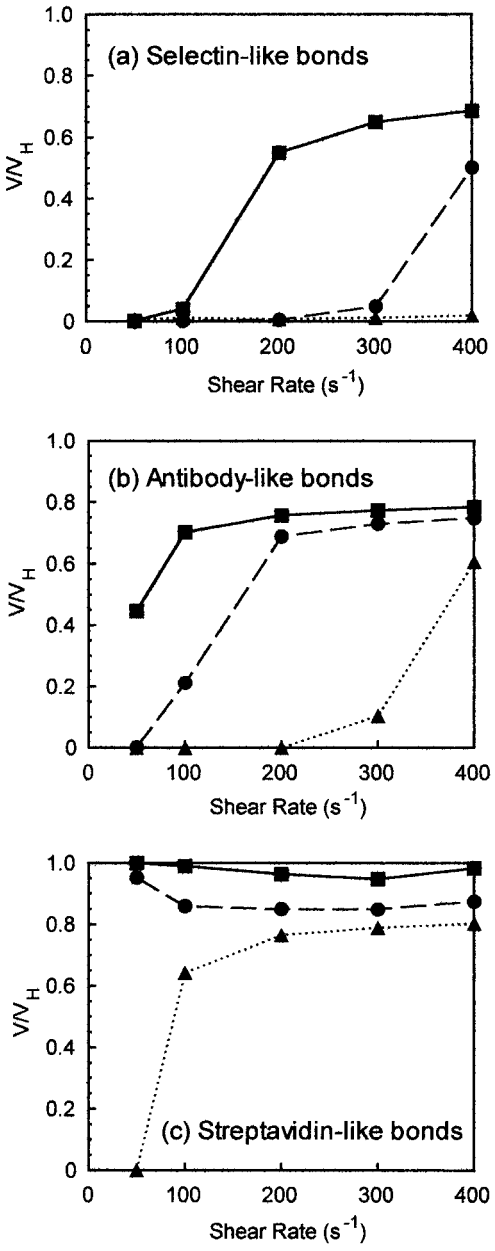

Figure 6. Graph of V/V_H versus shear rate for R_c = 5.0 μm (squares, solid line), 3.75 μm (circles, dashed line), and 2.5 μm (triangles, dotted line) at constant N_r. The different graphs represent the R_c curves for (a) selectin-like bonds (k_r^o = 1 s^{-1}, r_o = 0.3 Å), (b) antibody-like bonds ($k_r^o = 10^{-2}$ s^{-1}, r_o = 1.0 Å), and (c) streptavidin-like bonds ($k_r^o = 10^{-4}$ s^{-1}, r_o = 3.0 Å).

Discussion

In previous computational work, we used adhesive dynamics to simulate the adhesion of a cell to a surface in flow as some of the biophysical parameters that govern receptor–ligand functional properties and the dynamics of adhesion were varied. The data can be summarized in a state diagram, a one-to-one map between the biophysical properties of adhesion molecules and different adhesive behaviors. Adhesive behaviors that were observed in previous simulations included sudden firm capture from flow, transient adhesion (rolling), and no adhesion. We varied the bond dissociative properties, association rate, elasticity, and shear rate and found that the unstressed dissociation rate, k_r^o, and the bond interaction length, r_o, are the most

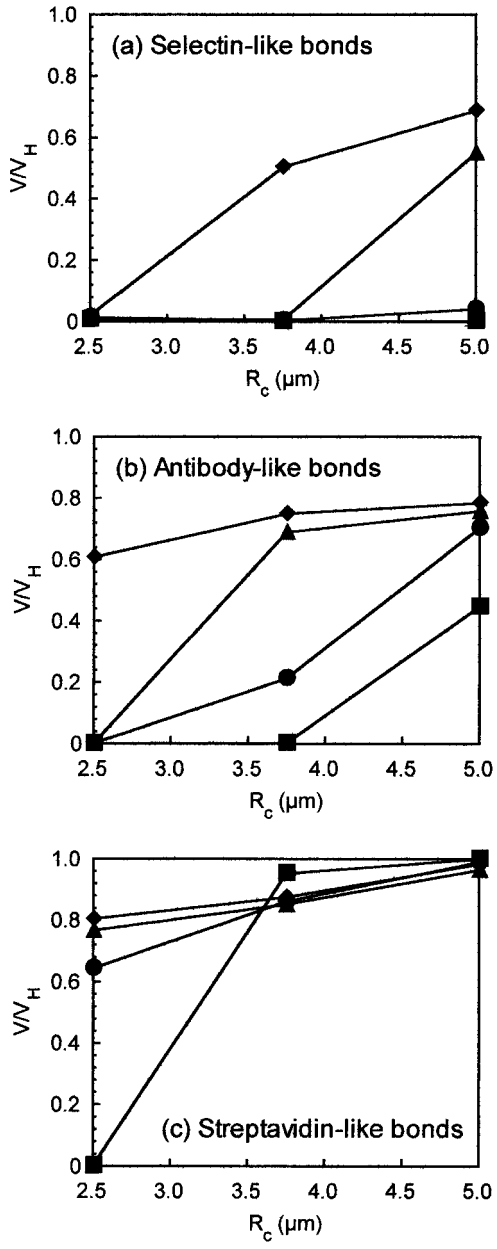

Figure 7. Graphs of the data in Figure 7a–c with V/V_H plotted versus R_c for $G = 50$ s^{-1} (squares), 100 s^{-1} (circles), 200 s^{-1} (triangles), and 400 s^{-1} (diamonds) at constant N_r. The different graphs represent the R_c curves for (a) selectin-like bonds ($k_r^o = 1$ s^{-1}, $r_o = 0.3$ Å), (b) antibody-like bonds ($k_r^o = 10^{-2}$ s^{-1}, $r_o = 1.0$ Å), and (c) streptavidin-like bonds ($k_r^o = 10^{-4}$ s^{-1}, $r_o = 3.0$ Å).

important molecular properties controlling the dynamics of adhesion. Experimental k_r^o and r_o values from the literature for molecules that are known to mediate rolling adhesion were seen to fall within the rolling region of the state diagram.

The present work shows the effect of varying the particle size on the state diagrams for adhesion. The work presented here shows that the overall shape of the state diagram does not change as particle size is varied, but shifts in the range of Bell model parameters that are needed for the rolling phenotype to be observed do occur. For smaller particles, larger values of r_o and k_r^o are needed to preserve the rolling velocity. This effect is reduced, but not eliminated, if the receptor density is held fixed, rather than the number of receptors.

The cell-free rolling experiments were performed using 10.5-μm-diameter particles, whereas neutrophils are closer to 8.5 μm in diameter.[14] The neutrophil size will thus fall between the results for 10- and 7.5-μm particles presented here. To see where parameter values that have been measured for selectin-mediated rolling lie on this state diagram, the values are plotted in Figure 2b. The points all lie near, or just slightly below, the curve for $0.0V_H$. A change of particle size to 8.5 μm will shift most of the experimental points back within the rolling region at this shear rate, and any further discrepancies in predictions of rolling behavior can be accommodated by modeling the specific experimental values for the forward reaction rate or receptor number used in the experiments in which the parameters were measured.

These state diagrams also illustrate another method for putting limits on the Bell model parameters associated with a given bond. Because the Bell model parameters should be independent of particle size, a set of experiments that measured V/V_H values for beads with different particle sizes at similar surface densities of adhesion molecules could be used to narrow down the region of r_o–k_r^o parameter space that can account for the observed behavior. Some predictions can be made. If it is possible to get beads of different sizes (covering a size range similar to that given here) to roll for the same density of receptors, then the Bell model parameter r_o is likely below 1 Å. This is because, for values greater than 1 Å, the width of the region for rolling adhesion is so narrow that, if the Bell model parameters for the interaction fall within the rolling envelope for one particle size, they would likely not fall within the corresponding diagram for a different size. For example, if 10-μm-diameter particles rolled, then 5.0-μm particles would be firmly adherent.

Recently, the Goetz lab has performed exactly the set of experiments required for finding limits on r_o by measuring the effect of bead size on rolling velocity.[36] They examined rolling at a range of shear stresses for 5-, 10-, 15-, and 20-μm beads and found that the bead rolling velocity increased with particle size at a given shear rate. They also determined that the critical shear stress for adherent beads to start rolling decreased with increasing bead size. The observation that rolling velocity increases as particle size increases is nontrivial because, although larger particles present a greater surface area to flowing fluid and hence experience larger drag forces, there are also increases in the contact area over which bonding is possible for larger particles. A spherical bead has a surface area, A ($= 2\pi h R_c$) within a distance, h, of a flat surface.[37,38] Given that h is fixed (because it is governed by the length of the receptor–ligand complex), as R_c increases, the contact area will also increase linearly, assuming that the bead maintains a fixed distance from the surface. This increase in contact area (which occurs even in the absence of cell deformability), along with surface roughness and changes in the bead–surface gap distance, can mitigate the effects of increasing drag force. The observations from the Goetz lab agree with the general trends shown in Figures 6 and 7, but additional work will be required to simulate the larger particles and determine which Bell model parameters fit the data best. Further simulations are also needed to examine the shear stress required to detach an already adherent cell (the experiment performed in Shinde Patil et al.).[36] The capture

shear stress at which a cell will adhere firmly to a substrate (as opposed to rolling slowly) from *flow* (the methodology of the current simulations) is not necessarily the same as the critical shear stress that will cause an already adherent cell to detach and roll. The shear stress at which the particle stops being firmly adherent and rolls, and then reattaches again after rolling, will likely be different if flow is turned up gradually and then turned down again. This rolling hysteresis effect will be the subject of future research.

The question arises as to whether is it possible to shift the location of the rolling or firm adhesion regions of the state diagram to any realistic set of Bell model parameter values by the use of a readily accessible experimental variable. One such variable is the particle size. From the standpoint of drug delivery, it should be possible to vary the particle size from perhaps 1 to 10 μm. For a given drug delivery particle size, one might wish to use an adhesion molecule that allows rolling at the shear rates and densities of adhesion molecules that are present in a given region of the circulation (shear rate varies with vessel size and pressure drop, and hence, it also varies with location in the vascular tree—shear rates in postcapillary venules are much lower than in arteries and larger veins, and there are also differences in selectin expression).[39,40] The simulations can indicate which Bell model parameters would be needed to mediate rolling (and hence enhanced residence time) for this bead size. Conversely, for a given choice of Bell model parameters, the model can give the range of shear rate for which a given particle size will be able to roll. These simulations show that it is not possible to move the rolling envelope drastically for a single shear rate by changing the particle size. It is, however, possible to change the rolling zone to a different range of shear rate and, hence, to allow the residence time for particles in an area of inflammation to be tuned.

Conclusions

In summary, previous simulations demonstrated that there is a family of state diagrams for which the shapes of the envelopes for rolling adhesion and firm arrest are similar but these envelopes shift depending on the value of the association rate, substrate ligand density, number of receptors on the cells, and exact experimental protocol. Our work illustrates how dynamic states of adhesion can be modified by tailoring the particle size to the problem. We demonstrate that Bell model parameters measured in the literature fall near the rolling region of the state diagram for the $R_c = 3.75$ μm, which is a more appropriate value for leukocyte. We also propose a method for obtaining limits on the Bell model parameters for an adhesion molecule by finding the parameters that best match cell-free adhesion experiments in flow with different sized beads.

Acknowledgment

This work was supported by NIH Grants HL18208 and OM59100 and a fellowship from the Fonds FCAR for D.F.J.T.

Literature Cited

(1) Springer, T. A. Traffic signals for lymphocyte recirculation and leukocyte emigration: The multistep paradigm. *Cell* **1994**, *76*, 301.

(2) Chang, K.-C.; Tees, D. F. J.; Hammer, D. A. The state diagram for cell adhesion under flow: Leukocyte rolling and firm adhesion. *Proc. Natl. Acad. Sci. U.S.A.* **2000**, *97*, 11262.

(3) Tempelman, L. A.; Hammer, D. A. Receptor-mediated binding of IgE sensitized rat basophilic leukemia cells to antigen-coated substrates under hydrodynamic flow. *Biophys. J.* **1994**, *66*, 1231.

(4) von Andrian, U. H.; Hasslen, S. R.; Nelson, R. D.; Erlandsen, S. L.; Butcher, E. C. A central role for microvillous receptor presentation in leukocyte adhesion under flow. *Cell* **1995**, *82*, 989.

(5) Brunk, D. K.; Goetz, D. J.; Hammer, D. A. Sialyl Lewis^x/E-selectin-mediated rolling in a cell-free system. *Biophys. J.* **1996**, *71*, 2902.

(6) Brunk, D. K.; Hammer, D. A. Quantifying rolling adhesion with a cell-free assay: E-selectin and its carbohydrate ligands. *Biophys. J.* **1997**, *72*, 2820.

(7) Rodgers, S. D.; Camphausen, R. T.; Hammer, D. A. Sialyl Lewis^x-mediated, PSGL-1-independent rolling adhesion on P-selectin. *Biophys. J.* **2000**, *79*, 694.

(8) Dembo, M.; Torney, D. C.; Saxman, K.; Hammer, D. The reaction limited kinetics of membrane-to-surface adhesion and detachment. *Proc. R. Soc. London B: Biol. Sci.* **1988**, *234*, 55.

(9) Evans, E.; Ritchie, K. Dynamic strength of molecular adhesion bonds. *Biophys. J.* **1997**, *72*, 1541.

(10) Bell, G. I. Models for the specific adhesion of cells to cells. *Science* **1978**, *200*, 618.

(11) Chen, S.; Springer, T. A. Selectin receptor−ligand bonds: Formation limited by shear rate and dissociation governed by the Bell model. *Proc. Natl. Acad. Sci. U.S.A.* **2001**, *98*, 950.

(12) Evans, E. Energy landscapes of biomolecular adhesion and receptor anchoring at interfaces explored with dynamic force spectroscopy. *Faraday Discuss.* **1998**, *111*, 1.

(13) Evans, E.; Ritchie, K. Strength of a weak bond connecting flexible polymer chains. *Biophys. J.* **1999**, *76*, 2439.

(14) Shao, J.-Y.; Ting-Beall, H. P.; Hochmuth, R. M. Static and dynamic lengths of neutrophil microvilli. *Proc. Natl. Acad. Sci. U.S.A.* **1998**, *95*, 6797.

(15) Alon, R.; Hammer, D. A.; Springer, T. A. Lifetime of the P-selectin−carbohydrate bond and its response to tensile force in hydrodynamic flow. *Nature (London)* **1995**, *374*, 539.

(16) Alon, R.; Chen, S.; Puri, K. D.; Finger, E. B.; Springer, T. A. The kinetics of L-selectin tethers and the mechanics of selectin-mediated rolling. *J. Cell Biol.* **1997**, *138*, 1169.

(17) Smith, M. J.; Berg, E. L.; Lawrence, M. B. A direct comparison of selectin-mediated transient adhesive events using high temporal resolution. *Biophys. J.* **1999**, *77*, 3371.

(18) Ramachandran, V.; Nollert, M. U.; Qiu, H.; Liu, W.-J.; Cummings, R. D.; Zhu, C.; McEver, R. P. Tyrosine replacement in P-selectin glycoprotein ligand-1 affects distinct kinetic and mechanical properties of bonds with P- and L-selectin. *Proc. Natl. Acad. Sci. U.S.A.* **1999**, *96*, 13771.

(19) Tees, D. F. J.; Waugh, R. E.; Hammer, D. A. A microcantilever device to assess the effect of force on the lifetime of selectin−carbohydrate bonds. *Biophys. J.* **2001**, *80*, 668.

(20) Frenette, P. S.; Johnson, R. C.; Hynes, R. O.; Wagner, D. D. Platelets roll on stimulated endothelium in vivo: An interaction mediated by endothelial P-selectin. *Proc. Natl. Acad. Sci. U.S.A.* **1995**, *92*, 7450.

(21) Savage, B.; Saldívar, E.; Ruggeri, Z. M. Initiation of platelet adhesion by arrest onto fibrinogen or translocation on von Willebrand factor. *Cell* **1996**, *84*, 289.

(22) Giavazzi, R.; Foppolo, M.; Dossi, R.; Remuzzi, A. Rolling and adhesion of human tumor cells on vascular endothelium under physiological flow conditions. *J. Clin. Invest.* **1993**, *92*, 3038.

(23) Goetz, D. J.; El-Sabban, M. E.; Hammer, D. A.; Pauli, B. U. Lu-ECAM-1 mediated adhesion of melanoma cells to endothelium under conditions of flow. *Int. J. Cancer* **1996**, *65*, 192.

(24) Morozov, V. N.; Morozova, T. Y. What does a protein molecule look like? *Commun. Mol. Cell. Biophys.* **1990**, *6*, 249.

(25) Hammer, D. A.; Apte, S. M. Simulation of cell rolling and adhesion on surfaces in shear flow: General results and analysis of selectin-mediated neutrophil adhesion. *Biophys. J.* **1992**, *63*, 35.

(26) Chang, K.-C.; Hammer, D. A. Influence of direction and type of applied force on the detachment of macromolecularly bound particles from surfaces. *Langmuir* **1996**, *12*, 2271.

(27) Kuo, S. C.; Hammer, D. A.; Lauffenburger, D. A. Simulation of detachment of specifically bound particles from surfaces by shear flow. *Biophys. J.* **1997**, *73*, 517.

(28) Chang, K.-C.; Hammer, D. A. Adhesive dynamics simulations of sialyl-Lewis^x/E-selectin-mediated rolling in a cell-free system. *Biophys. J.* **2000**, *79*, 1891.

(29) Chang, K.-C.; Hammer, D. A. The forward rate of binding of surface-tethered reactants: Effect of relative motion between two surfaces. *Biophys. J.* **1999**, *76*, 1280.

(30) Goldman, A. J.; Cox, R. G.; Brenner, H. Slow viscous motion of a sphere parallel to a plane wall. II. Couette flow. *Chem. Eng. Sci.* **1967**, *22*, 653.

(31) Lawrence, M. B.; McIntire, L. V.; Eskin, S. G. Effect of flow on polymorphonuclear leukocyte/endothelial cell adhesion. *Blood* **1987**, *70*, 1284.

(32) Lawrence, M. B.; Smith, C. W.; Eskin, S. G.; McIntire, L. V. Effect of venous shear stress on CD18-mediated neutrophil adhesion to cultured endothelium. *Blood* **1990**, *75*, 227.

(33) Chen, S.; Springer, T. A. An automatic braking system that stabilizes leukocyte rolling by an increase in selectin bond number with shear. *J. Cell Biol.* **1999**, *144*, 185.

(34) Fritz, J.; Katopodis, A. G.; Kolbinger, F.; Anselmetti, D. Force-mediated kinetics of single P-selectin/ligand complexes observed by atomic force microscopy. *Proc. Natl. Acad. Sci. U.S.A.* **1998**, *95*, 12783.

(35) Alon, R.; Chen, S.; Fuhlbrigge, R.; Puri, K. D.; Springer, T. A. The kinetics and shear threshold of transient and rolling interactions of L-selectin with its ligand on leukocytes. *Proc. Natl. Acad. Sci. U.S.A.* **1998**, *95*, 11631.

(36) Shinde Patil, V. R.; Campbell, C. J.; Yun, Y. H.; Slack, S. M.; Goetz, D. J. Particle diameter influences adhesion under flow. *Biophys. J.* **2001**, *80*, 1733.

(37) Tha, S. P.; Goldsmith, H. L. Interaction forces between red cells agglutinated by antibody I. Theoretical. *Biophys. J.* **1986**, *50*, 1109.

(38) Tees, D. F. J.; Goldsmith, H. L. Kinetics and locus of failure of receptor−ligand-mediated adhesion between latex spheres. I. protein−carbohydrate bond. *Biophys. J.* **1996**, *71*, 1102.

(39) Nichols, W. W.; O'Rourke, M. F. *McDonald's Blood Flow in Arteries: Theoretical, Experimental, and Clinical Principles*, 3rd ed.; Lea & Febiger: Philadelphia, PA, 1990.

(40) Ley, K.; Gaehtgens, P. Endothelial, not hemodynamic, differences are responsible for preferential leukocyte rolling in rat mesenteric venules. *Circ. Res* **1991**, *69*, 1034.

Received for review April 27, 2001
Revised manuscript received October 3, 2001
Accepted October 5, 2001

IE010383P